# A User Interface for a Seven Degree of Freedom Surgical Robot

*J.S. Heunis[a], C. Scheffer[a] and K. Schreve[a]*

Received 25 January 2013, in revised form 30 April 2013 and accepted 30 September 2013

***This paper presents the design of a joystick-type user interface for the master-slave control of a seven degree of freedom (DOF) minimally invasive surgical robot. The joystick is a seven DOF all revolute articulated arm. The electronic design implements AS5040 magnetic rotary encoders for the joystick's position and orientation tracking. The control system required the mathematical modelling of the joystick and robot using the Denavit-Hartenberg convention. Testing demonstrates the intuitiveness of the joystick control.***

**Additional keywords:** BERG, MIS, MIRS, MEMS

## Nomenclature

### Roman

| | |
|---|---|
| $a$ | Link length |
| $A$ | Transformation matrix |
| $d$ | Link offset |
| $M$ | Referring to the master reference frame |
| $o$ | Origin of a three-dimensional reference frame |
| $p$ | A point in a three-dimensional reference frame |
| $q$ | Joint variable |
| $R$ | Rotation matrix |
| $S$ | Referring to the slave reference frame |
| $T$ | Transformation matrix |

### Greek

| | |
|---|---|
| $\alpha$ | Link twist |
| $\theta$ | Joint angle |

### Abbreviations

| | |
|---|---|
| CCW | Counter Clockwise (w.r.t. motor output shaft) |
| CW | Clockwise (w.r.t. motor output shaft) |
| CAD | Computer Aided Drawing |
| DH | Denavit-Hartenberg |
| DOF | Degree(s) of Freedom |
| GUI | Graphical User Interface |
| IDE | Integrated Development Environment |
| MEMS | Micro-electrical Mechanical Systems |
| MIRS | Minimally Invasive Robotic Surgery |
| MIS | Minimally Invasive Surgery |
| PCB | Printed Circuit Board |
| PSM | Primary Slave Manipulator |
| PWM | Pulse Width Modulation |
| SPI | Serial Peripheral Interface |
| SSI | Serial Synchronous Interface |
| SSM | Secondary Slave Manipulator |

a Biomedical Engineering Research Group (BERG), Department of Mechanical and Mechatronic Engineering, Stellenbosch University, Stellenbosch, South Africa. Tel.: +27 (21) 808 4249, E-mail: cscheffer@sun.ac.za

## 1. Introduction

The process of minimally invasive surgery (MIS) allows surgeons to operate on patients without having to make the large incisions that are necessary with conventional surgical methods. The small incision length contributes to several positive factors: improved survival statistics, fewer post-surgical complications, shortening of the patient recovery period and a quicker return to normal life[1]. A typical wound from a traditional surgical incision may require a six-week recovery period[2]; on the other hand, the recovery time for a laparoscopic hysterectomy is more or less two weeks. This greatly reduces the recovery (and therefore inactive) period for the patient while simultaneously decreasing hospitalization time and thus costs.

The implementation of computer and robot-assisted surgical procedures has developed so well that currently, more than 1000 surgical robots are in regular clinical use worldwide and research and development is done at more than 100 universities[3]. The use of surgical robots for laparoscopic surgery ensures enhanced dexterity, more degrees of freedom for tool movement, better visual feedback to the surgeon (by using cameras and visual displays) and ultimately positive increases in all of the advantages provided by MIS.

Minimally invasive robotic surgery (MIRS) has the ability to reduce human error. Through programming the correct interface the surgical tool will have the ability to carry out the precise movements made by the surgeon at the master console, which effectively avoids the reverse-fulcrum-induced movements of normal MIS[4]. Further additions to the system are also enabled with the use of robotics. Advances in the area of micro-electrical mechanical systems (MEMS) point to the use of miniature sensors and actuators to enable haptic feedback in the robot, and high-fidelity force sensors can be used to improve force sensation beyond what the human hand can sense on its own[4].

As part of a surgical robot project for the Biomedical Engineering Research Group (BERG) at Stellenbosch University, Christiane[5] developed a four degree of freedom (DOF) primary slave manipulator (PSM) that is responsible for manipulating its main surgical tool. In addition to that, Worst[6] developed the secondary slave manipulator (SSM) that is responsible for controlling the primary manipulator as well as adding another three DOF to the system. This gives the robot a total of seven degrees of freedom and makes it comparable with the seven DOF Da Vinci system from Intuitive Surgical[7]. In this paper, the design and construction of the user interface for the existing robot is presented.

Literature shows that different methods for master controller design exist in the surgical robot environment, with Simorov *et al.*[8] providing a thorough overview of current technologies. The design of the user interface

  

mainly depends on the specific attributes of the existing slave robot as well as solution-specific requirements.

Tavakoli *et al.*[9], for example, developed a system incorporating an existing laparoscopic surgical tool in conjunction with the 6 DOF Phantom Premium haptic tool from SensAble Technologies[10]. Because the surgical tool pivots around the point where it enters the patient through the incision (the trocar is the tool used to create and hold this incision), the conventional MIS surgeon has to make opposite movements to obtain the correct tool positioning. This phenomenon, known as the fulcrum effect, is often seen as a major drawback of MIS and is therefore normally absent in most MIRS systems.

Another attractive option in surgical robot master console design is to develop a user interface that has the same geometry (although scaled down in size) as the actual robot, as was done with the MASTER transluminal endoscopic robot at Nanyang Technological University[8,11]. This allows for less complicated position tracking and control system design, because the actuators of the robot would only have to execute the same (scaled down) movements as experienced by the respective links on the master system. One drawback here is the fact that such a design restricts the master console to only being used for that specific project. If a design change is necessary at the slave end of the system, the master also has to be changed accordingly. The versatility of the interface is thus limited, which is why many current MIRS systems follow a more generic approach where the requirement is only to provide enough DOF in order for the surgeon to move the end-tool to the correct position and orientation necessary at the robot tool end. Examples include the MiroSurge robot from DLR Institute of Robotics and Mechatronics[8], the RAVEN surgical system from UCSC[8], SOFIE from the Eindhoven University of Technology[12] and the Da Vinci system[7].

Another user interface type entails the use of so-called data gloves in conjunction with a virtual reality platform, like the prototype designed by CyberGlove II Systems LLC in San Jose[8]. Sensors on the glove detect movement of fingers and hands relative to each other and relative to a global reference frame, thus allowing control of the robot manipulator. Visual feedback is also provided to the operator to such an extent that he/she will feel fully immersed in the surgical environment. This method can provides accurate, three dimensional and real-time feedback but lacks the framework with which effective haptick/force feedback can be provided, which is where manipulator user interfaces like that of the Da Vinci system have the advantage. Although not all provided examples make use of haptic feedback, the physical platform is already established and can be expanded on. The introduction of haptic feedback to data gloves is, however, not excluded, with Simorov *et al.*[8] proposing the use of vibratory sensors towards this purpose.

## 2. The Slave System

The existing slave consists of two parts: the primary slave manipulator (PSM)[5] and the secondary slave manipulator (SSM)[6], both shown below in figure 1 and figure 2 respectively. Figure 3 shows the assembled slave manipulator.

The PSM has a typical spherical wrist design (three revolute joints in a specific configuration[13]) with an added gripper, which constitutes its fourth DOF. The SSM consists of three joints, with a revolute-revolute-prismatic configuration, that form the three base degrees of freedom of the slave manipulator.

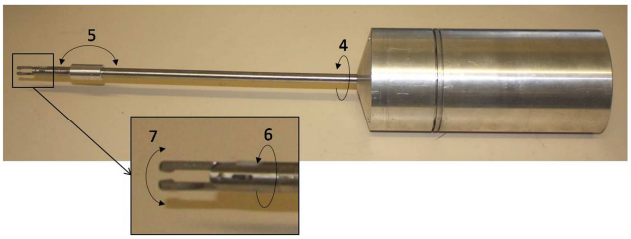


Figure 1: The PSM with its degrees of freedom indicated

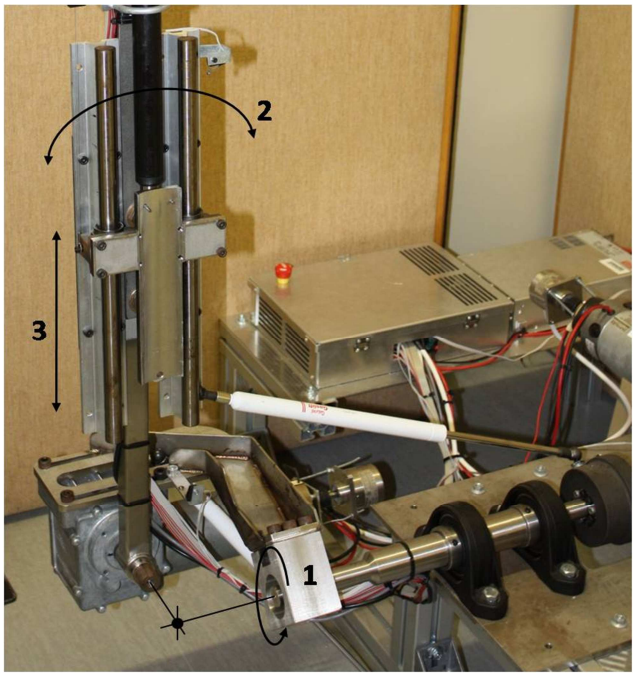


Figure 2: The SSM with its degrees of freedom indicated

Figure 1 and figure 2 indicate that the PSM's degrees of freedom are numbered 4, 5, 6 and 7 and that those of the SSM are numbered 1, 2 and 3. This was done in order to conserve the convention that is followed throughout this paper: the surgical robot's degrees of freedom start at 1 at the base motor of the SSM, after which they follow on each other in numerical order up to DOF 7, the gripper.

The SSM was designed in such a way that the actuation axes of joints 1, 2 and 3 all intersect at one point (indicated in figure 2). When the PSM is fitted to the main assembly, the axes of joints 3 and 4 coincide, which results in the main tool shaft passing through the said intersection point. This was intentionally designed so as to provide an entrance point for the surgical robot into the trocar in the patient's body. Once the robot is in the correct position, any actuation of joints 1, 2, 3 and 4 would cause the end effector to move but the physical position of the tool

insertion point would be unaltered and the patient will be unharmed.

The slave system joint numbers, their manner of operation and their specific constraints are given in table 1 below.

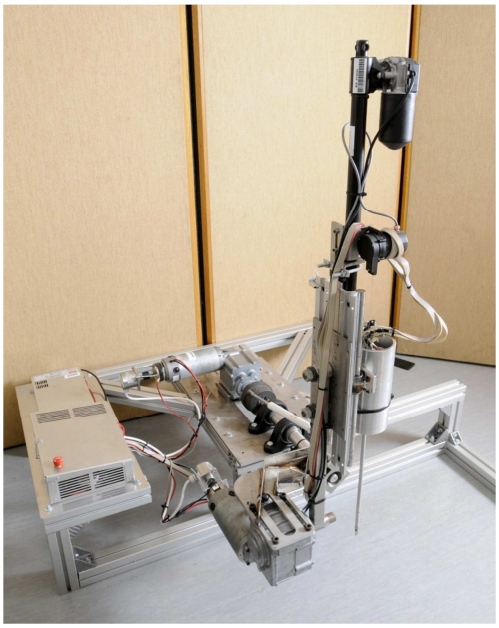

Figure 3: The assembled slave system

Table 1: Slave system joint specifics

| DOF | Description |
|---|---|
| 1 | The base joint rotates about a horizontal axis. When looking at the robot from the front right position, and regarding the second link of the robot in the upright position (as indicated in figure 2), actuation of joint 1 can result in a 11° CCW rotation and a 30° CW rotation due to physical constraints of the design. |
| 2 | This joint rotates about an axis perpendicular to DOF 1. When regarding the robot from the front and right hand side, again considering the second link in the upright position, actuation of this joint can result in a 11° CCW rotation and a 24° CW rotation, due to physical constraints of the design. |
| 3 | This is the only prismatic joint in the whole kinematic chain. The linear motor is attached to the second link (used as the reference above) and allows a 283 mm stroke length from the topmost position. |
| 4 | The main PSM shaft rotates about its own longitudinal axis. 360° rotation is possible. |
| 5 | The distal part of the main PSM shaft beyond the elbow joint can rotate 55° from the extended position (where the distal part's axis is in line with the joint 4 axis) to the extreme flexion position. The physical aspects of the design do not allow further rotation. |
| 6 | The front part of the shaft can rotate 90° about the distal shaft axis, due to physical design constraints. |
| 7 | The gripper constitutes the final joint. It can open and close. |

## 3. Requirements

The main objective was to develop a user interface for the seven DOF minimally invasive surgical robot consisting of the PSM and SSM. This problem was divided into several subsections listed below:

- To design and construct a mechanical joystick that the surgeon can use to control the movement of the seven DOF surgical tool.
- To design and implement the encoder system that is used to track the surgeon's hand movements.
- To design and implement the necessary electronics that allows the mechanical, electronic and encoder components of the joystick to work together as one system.
- To implement an effective communication system between the master console and the collective PSM and SSM system.
- To design the control system that will regulate how the joystick is able to control the surgical tool.
- To design and conduct experiments to test the working of the control system and the accuracy with which the robot's movements are controlled.

From these objectives, and throughout the course of the different design sections, several engineering specifications were derived. The list below shows the final set of engineering specifications that the end-product had to satisfy:

- The joystick should be designed to be controlled with only one hand.
- The user interface should provide an unhindered movement space of 30 cm x 30 cm x 30 cm, allowing a downscaling factor of 3:1 [14].
- The encoders should be small and lightweight, preferably custom solutions rather than bulky commercial encoders.
- The combined encoder resolution of the user interface should be 9 mm in order to satisfy the surgical robot resolution requirement.
- The combined encoder resolution of the user interface should be 0.9 mm in order to satisfy the suture resolution requirement.
- The design should allow a 'safe space' volume of 10 cm x 10 cm x 10 cm for the movement of the robot end effector.
- The joystick's base frame should not experience more than 1 mm deflection and the combined link deflection of the kinematic chain should not be more than 0.6 mm.
- It must be possible to actuate the joystick joints separately from each other, while keeping the applicable joints stationary. This is to enable direct 'DOF to DOF' control of the PSM motors.
- A safety switch should be incorporated with the following requirements: when pressed, the joystick should be able to control the robot's movement; when released, the robot should not execute any movement occurring at the joystick side.

 

- Minimal mass should be carried by the operator while operating the joystick.
- The movement of the joystick's end effector should directly be translated to the movement of the robot end effector, taking the scaling factor into account.
- Detailed knowledge of how the joystick is designed and how it functions should not be a prerequisite to being able to operate it.

## 4. Mechanical Design

The joystick was designed to have six revolute joints that form a kinematic chain hanging down from the base frame. It is shown in figure 4a, with the two base parts, the gripper and all degrees of freedom indicated. The long arms of the two base parts can slide over each other in order to adjust the height of the system.

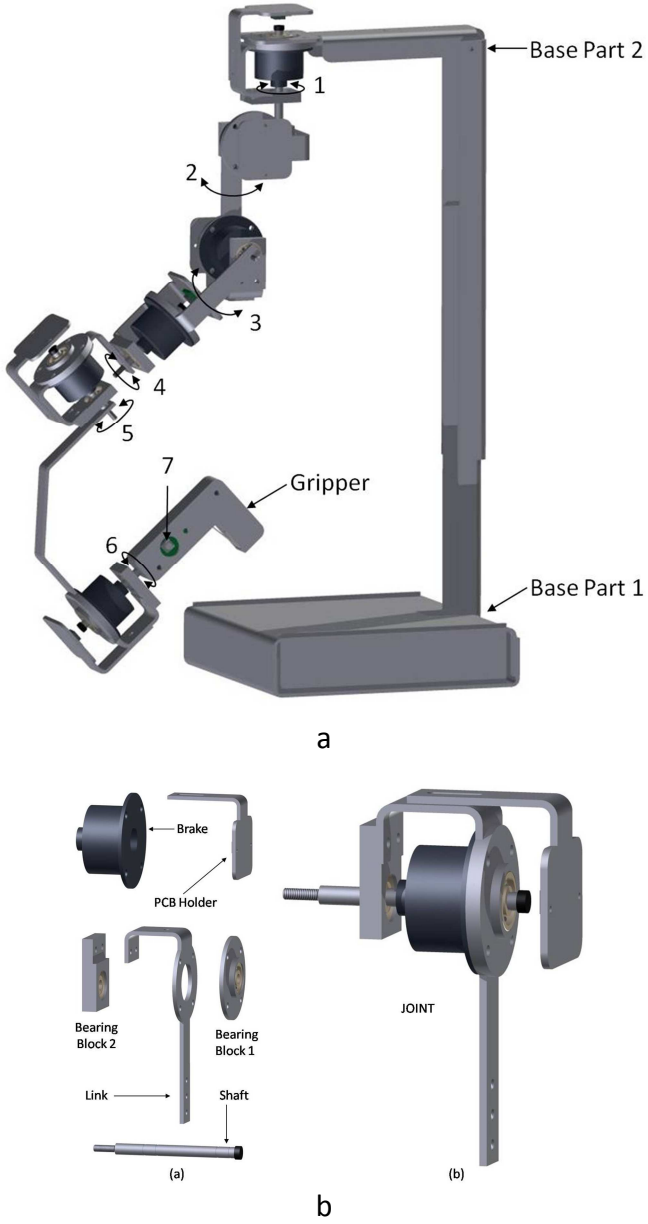


Figure 4: (a) The mechanical joystick design
(b) The basic joint design

A U-shape profile was used for the extensions of the base parts to create a strong frame that is able to hold the mass of all the joints and experiences less than the allowed deflection. Aluminium sheet metal was used for the 400 mm high frame and all other manufactured parts, in order to keep the mass minimal while conserving system rigidity.

The basic functional unit of the joystick, the joint, has a standard design (shown in figure 4b) which was used for every DOF of the master. The link forms the base part of the assembly and two bearing blocks are bolted to the link, with the rotating shaft inserted through the bearings. The end of each shaft serves as the fixing place for the next joint in the kinematic chain; at the end of the sixth joint's shaft, the gripper part is fixed. The gripper part was designed to be held by the operator during surgery. It contains two pushbuttons that have to be pressed simultaneously in order to actuate the slave's gripper, as well as a safety switch that satisfies the movement translation requirement mentioned in the requirements section above.

To allow individual joints to be operated separately, or to hold the position of the joystick stationary at any time, an electromagnetic brake (Miki-Pulley 112-02-11[15]) was included in each of the master's first six joint designs.

Finally, the joint features a fixed printed circuit board (PCB) holder which holds the movement tracking circuitry for each joint. Figure 5 shows the assembled joystick.

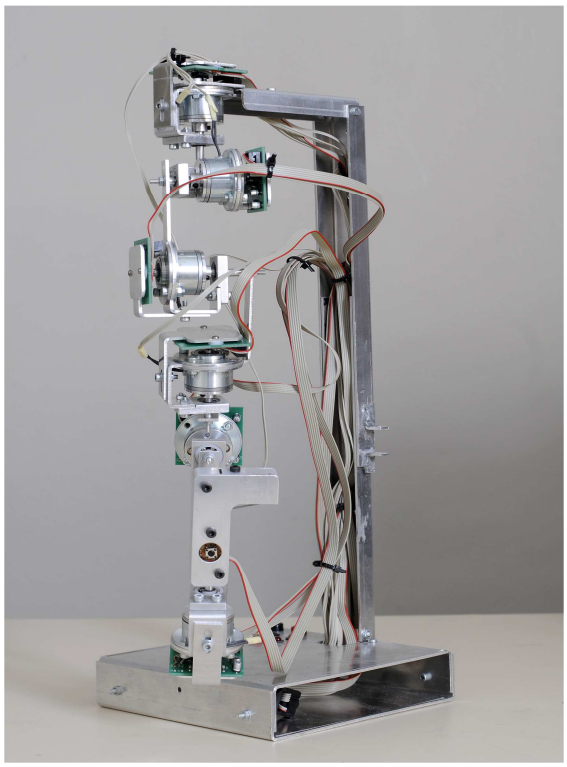

Figure 5: The assembled joystick

## 5. Electronic Design

The objectives that influenced the joystick's electronic development stated the need to design the encoder system and to implement electronics enabling the combined functioning of the joystick components. An effective communication system within the master setup, as well as between the master and the slave, was also necessary.

These aspects can be summarized conceptually as system inputs, system outputs and the main controller that regulates everything in between. Figure 6 shows these relationships diagrammatically.

A 10 bit rotary magnetic encoder chip (AS5040 from Austria Microsystems[16]), along with the accompanying magnet, was incorporated for position and orientation tracking. The magnet was fixed to the end of the shaft (see figure 4b) and the encoder chip, sensing the rotation, produces 1024 pulse outputs per revolution on two quadrature output lines. A lightweight custom PCB (mounted on the holder indicated in figure 4b) was designed to enable quadrature sensing and to minimize the mass carried by the operator.

To control the existing robot, an Arduino Mega 2560 development board[17] was already in place. To simplify interfacing procedures, the same control board was chosen as the master controller.

The final aspects indicated in figure 6 included setting up tactile switches for the gripper and toggle switches to control the electromagnetic brakes.

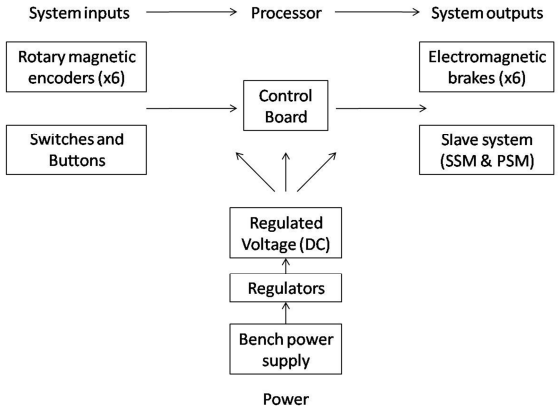


Figure 6: The electronic specifications diagram for the joystick

## 6. Master And Slave Interfacing

In order for the main objectives pertaining to master-slave control to be satisfied, the master and slave systems had to be interfaced correctly. Firstly, the PSM and SSM systems had to function correctly according to requirements from the master side, which included the correct functioning of each motor and encoder in the PSM and SSM and the ability to communicate with the central control board of the surgical robot. Where necessary, adjustments or changes had to be made. Then, there had to be a centre of control with which the master system could communicate. Once these aspects were set up, communication and control could be executed.

This interfacing process brought several shortcomings of the slave system to light, mostly as a result of fundamental errors in the mechanical designs of the PSM and SSM. The PSM's motors were over-specified and the spherical wrist design was inadequate, leading to its joint cables breaking at critical moments during robot operation, while the big and heavy components on the SSM produced excessive torque levels that were hard to overcome. Where possible, these aspects were accounted for by making adjustments or changes, but the final result was that seven DOF control could not be demonstrated on the slave. This aspect is discussed further in the control section.

Despite these hindrances, the master and slave interfacing process successfully established a direct serial communication line at a baud rate of 9600 bits/s. All motor control instructions to, and encoder data from, the PSM and SSM were relayed along wires connected to the central slave control board. Instructions to the slave were sent along the serial communication line from the master control board.

## 7. Modelling

Both the master and slave systems were modelled according to the Denavit-Hartenberg convention as presented by Spong *et al.*[13]. With the DH convention, a manipulator is modelled according to a certain set of rules, specifically with regards to how the coordinate frames are defined. If it is assumed that the first coordinate frame is denoted $o_0x_0y_0z_0$, the three basic DH principles are as follows:

(DH0) The $z$-axis of each frame should be the axis of rotation/translation.

(DH1) The axis $x_1$ should be perpendicular to the axis $z_0$, i.e. $x_i$ should be perpendicular to $z_{i-1}$.

(DH2) The axis $x_1$ should intersect the axis $z_0$, i.e. $x_i$ should intersect $z_{i-1}$.

The resulting models are shown below in figure 7 and in figure 8 respectively. For clarification a superscript is used, where applicable, to denote the reference frame, while a subscript denotes the frame that applies to the indicated point, vector or matrix.

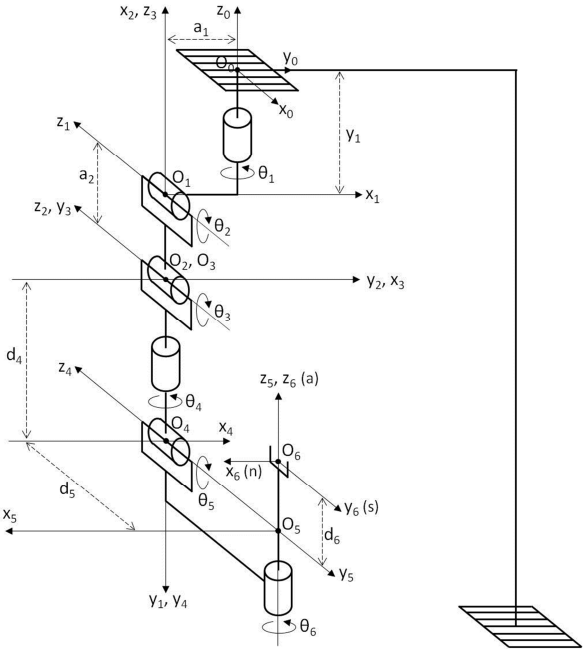


Figure 7: The joystick (master) model based on DH-principles

In these models, an $o_ix_iy_iz_i$ coordinate system is defined for each DOF, while the link length ($a_i$) and link twist ($\alpha_i$) are

constants determined by the physical aspects of the master and slave links. The joint variables are $\theta_i$ for the rotational joints and $d_i$ for the prismatic joints.

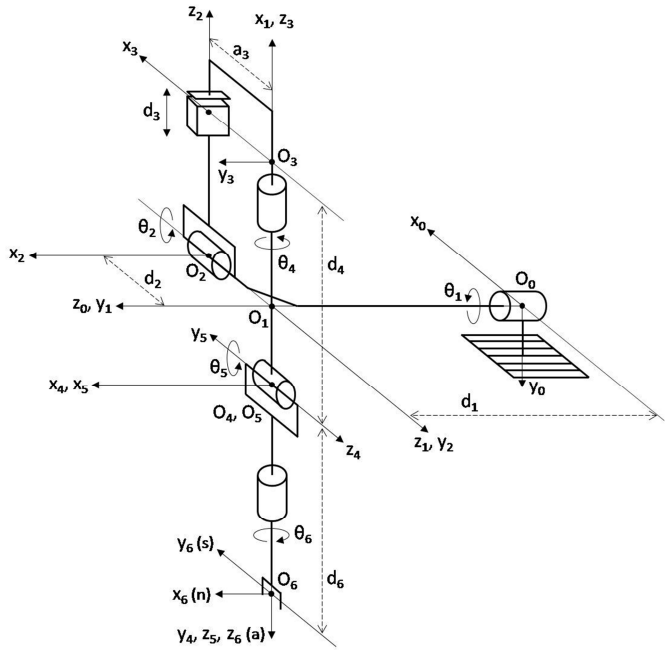


Figure 8: The robot (slave) model based on DH-principles

According to the DH convention, $\theta_i$ is measured from $x_{i-1}$ to $x_i$, which implies that $\theta_i$ is zero when axes $x_{i-1}$ and $x_i$ are parallel and in the same direction. It is evident from figure 7 and figure 8 that the models were not set up in this way – rather, the starting values were chosen to show the joystick robot in an easily understandable manner, thereby simplifying the models' interpretation. These starting values are given in table 2 and table 3 below. Table 4 and table 5 give the link and joint variables of the respective models, with the asterisk indicating variable values.

Table 2: Starting joint variable values for the joystick model

| $\theta_1$ | $\theta_2$ | $\theta_3$ | $\theta_4$ | $\theta_5$ | $\theta_6$ |
|---|---|---|---|---|---|
| 90° | -90° | 90° | 0° | 180° | 0° |

Table 3: Starting joint variable values for the robot model

| $\theta_1$ | $\theta_2$ | $d_3$ | $\theta_4$ | $\theta_5$ | $\theta_6$ |
|---|---|---|---|---|---|
| -90° | 90° | 528 mm | 90° | 0° | 0° |

## 8. Control

### 8.1 Kinematics

Control was executed at a rate of 50 Hz by the two Arduino Mega 2560 control boards. The primary objective here was to have the robot end effector carry out the same movement as experienced by the joystick end effector, subject to scaling and axis alignment operations. Thus, when the orientation and position of the joystick's end effector are known, the required orientation and position of the robot end effector (recalculated according to scaling and other factors) should be known, and instructions could be sent to the robot motors to move to this position and orientation. This process is diagrammatically indicated in figure 9.

Table 4: The joystick link and joint variables

| Link | $a_i$ (mm) | $\alpha_i$ | $d_i$ (mm) | $\theta_i$ |
|---|---|---|---|---|
| 1 | -20 | -90° | -60.8 | $\theta_1^*$ |
| 2 | -65 | 0° | 0 | $\theta_2^*$ |
| 3 | 0 | 90° | 0 | $\theta_3^*$ |
| 4 | 0 | -90° | -118.5 | $\theta_4^*$ |
| 5 | 0 | -90° | -95.3 | $\theta_5^*$ |
| 6 | 0 | 0° | -27.6 | $\theta_6^*$ |

Table 5: The robot link and joint variables

| Link | $a_i$ (mm) | $\alpha_i$ | $d_i$ (mm) | $\theta_i$ |
|---|---|---|---|---|
| 1 | 0 | 90° | 682 | $\theta_1^*$ |
| 2 | 0 | 90° | -176 | $\theta_2^*$ |
| 3 | -162 | 0° | $d_3^*$ | -90° |
| 4 | 0 | -90° | -520 | $\theta_4^*$ |
| 5 | 0 | -90° | 0 | $\theta_5^*$ |
| 6 | 0 | 0 | 50 | $\theta_6^*$ |

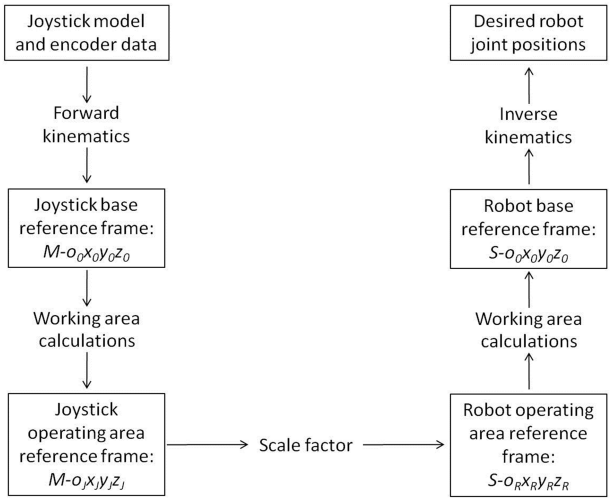


Figure 9: The master-slave control setup

To produce constantly known values for the positions of all joystick and robot joints, joint zero positions were determined and incorporated according to the models of figure 7 and figure 8 and the values in table 2 through table 5. The forward kinematic equations[13] for the joystick were then calculated to produce independent transformation matrices applicable to each reference frame ($A_i$) and transformations matrices of one reference frame in terms of another ($T_i$). The standard equations are indicated below.

$A_1$ to $A_6$ were determined according to equation 1, which enabled $T_6^0$, $R_6^0$ and $o_6^0$ to be calculated according to equation 2. These quantities gave the position and orientation of the joystick's end effector with respect to its base reference frame, $M\text{-}o_0x_0y_0z_0$. To enable direct movement translation from the master to the slave, the joystick and robot working volumes ($M\text{-}o_J x_J y_J z_J$ and $S\text{-}o_R x_R y_R z_R$ respectively) were created and orientated identically, as shown in figure 10. The position and orientation in the joystick's base reference frame were

transformed to the same entities in the $o_J x_J y_J z_J$ reference frame, which were then scaled down to find the required position and orientation of the robot end effector in the $o_R x_R y_R z_R$ reference frame. The equations used for these steps are given below figure 10.

$$A_i = \begin{bmatrix} \cos\theta_i & -\sin\theta_i \cos\alpha_i & \sin\theta_i \sin\alpha_i & a_i \cos\theta_i \\ \sin\theta_i & \cos\theta_i \cos\alpha_i & -\cos\theta_i \sin\alpha_i & a_i \sin\theta_i \\ 0 & \sin\alpha_i & \cos\alpha_i & d_i \\ 0 & 0 & 0 & 1 \end{bmatrix} \quad (1)$$

$$T_j^i = A_{i+1} A_{i+2} \cdots A_{j-1} A_j = \begin{bmatrix} R_j^i & o_j^i \\ 0 & 1 \end{bmatrix} \quad (2)$$

$$X_J = o_6^0(X) - X_{j0} \quad (3)$$

$$Y_J = o_6^0(Z) - Z_{j0} \quad (4)$$

$$Z_J = Y_{j0} - o_6^0(Y) \quad (5)$$

$$(X, Y, Z)_R = (X, Y, Z)_J / 3 \quad (6)$$

$$X = X_{r0} - X_R \quad (7)$$

$$Y = Y_{r0} - Y_R \quad (8)$$

$$Z = Z_R + Z_{r0} \quad (9)$$

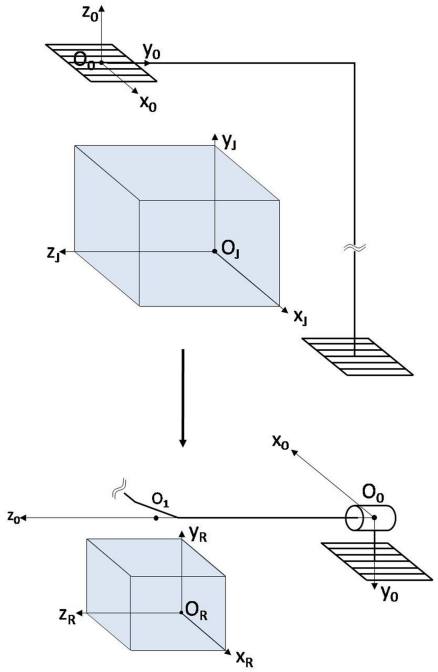


Figure 10: The master and slave working volumes

$$R_J = \left(R_J^0\right)^T R_6 R_J^0 = \begin{bmatrix} 1 & 0 & 0 \\ 0 & 0 & 1 \\ 0 & -1 & 0 \end{bmatrix} R_6 \begin{bmatrix} 1 & 0 & 0 \\ 0 & 0 & -1 \\ 0 & 1 & 0 \end{bmatrix} \quad (10)$$

$$R_R = R_J \quad (11)$$

$$R_6 = \left(R_0^R\right)^T R_J R_0^R = \begin{bmatrix} -1 & 0 & 0 \\ 0 & -1 & 0 \\ 0 & 0 & 1 \end{bmatrix} R_J \begin{bmatrix} -1 & 0 & 0 \\ 0 & -1 & 0 \\ 0 & 0 & 1 \end{bmatrix} \quad (12)$$

Equations 3 through 9 were used to determine the required robot end effector position from the known joystick end effector position, while equations 10 through 12 were used similarly for the orientations. The values of $(X, Y, Z)_{j0}$ and $(X, Y, Z)_{r0}$ in the equations above refer to the respective distances from the origin of the joystick and robot base frames to the origins of the joystick and robot working volume frames. The $(X, Y, Z)_{r0}$ values stay constant throughout operation and were chosen to position the robot working area directly beneath the virtual fulcrum point denoted by $o_1$ in figure 8.

The $(X, Y, Z)_{j0}$ values for the joystick, however, changed constantly due to the specific implementation of the safety button functionality. To keep the robot stationary while the safety switch is released and to move the robot from that precise stationary point when the safety switch is pressed, a new algorithm was developed. It keeps the joystick working volume locked to the joystick's end effector while the

safety switch is pressed and it locks the joystick working volume with respect to the base frame while the switch is released. This implies that movement inside the joystick working volume (which directly translates to the movement inside the robot working volume) is only registered when the safety switch is pressed. No precedence of such an algorithm was found in literature and as such it is declared a novel aspect.

The inverse kinematic calculations to determine the robot joint variables followed a kinematic decoupling[13] process whereby the slave joints were mathematically decoupled into a spherical wrist and three base joints. First, the wrist centre was found by using equations 13 through 15, after which the first three joint variables were calculated with equations 16 through 21.

$$X_C = X - d_6\, r_{13} \tag{13}$$

$$Y_C = Y - d_6\, r_{23} \tag{14}$$

$$Z_C = Z - d_6\, r_{33} \tag{15}$$

$$\theta_1 = \begin{cases} -\left|\tan^{-1}\left(\frac{X_C}{Y_C}\right)\right|, & if\ X_C \le 0 \\ \left|\tan^{-1}\left(\frac{X_C}{Y_C}\right)\right|, & if\ X_C > 0 \end{cases} \tag{16}$$

$$r = \sqrt{(X_C)^2 + (Y_C)^2} \tag{17}$$

$$s = Z_C - d_1 \tag{18}$$

$$\theta_2 = \begin{cases} \left|\tan^{-1}\left(\frac{S}{r}\right)\right|, & if\ s < 0 \\ -\left|\tan^{-1}\left(\frac{S}{r}\right)\right|, & if\ s \ge 0 \end{cases} \tag{19}$$

$$d_R = \sqrt{(r)^2 + (s)^2} \tag{20}$$

$$d_3 = d_4 - d_R \tag{21}$$

In the above equations, the value of $d_6$ was given in table 5 and the $r_{13}$ to $r_{33}$ values refer to the specific indices of the required *S*-$R_6$ matrix (with *S* referring to the slave) calculated with equation 12. With the first three robot joint variables known, *S*-$A_1$ to *S*-$A_3$ were determined according to equation 1, which enabled S-$T_1^0$ to S-$T_2^0$ to be calculated with equation 2. The rotation matrix *S*-$R^0_3$ was then derived from S-$T_2^0$ and was used in equation 22:

$$S\_R_6^3 = (S\_R_3^0)^T\, S_{R_6}. \tag{22}$$

From this, the final robot joint variables were calculated as the following set of Euler angles[12]:

$$\theta_4 = \begin{cases} \tan2^{-1}\left(r_{33}, \sqrt{1-(r_{33})^2}\ \right)\ or \\ \tan2^{-1}\left(r_{33}, -\sqrt{1-(r_{33})^2}\ \right) \end{cases} \tag{23}$$

$$\theta_5 = \begin{cases} \tan2^{-1}(\,r_{13},\, r_{23})\ or \\ \tan2^{-1}(-\,r_{13},\, -\,r_{23}) \end{cases} \tag{24}$$

$$\theta_6 = \begin{cases} \tan2^{-1}(-\,r_{31},\, r_{32})\ or \\ \tan2^{-1}(r_{31},\, -\,r_{32}) \end{cases} \tag{25}$$

In the above calculations, the $r_{13}$ to $r_{33}$ values refer to the specific indices of the S_$R_6^3$ matrix. With these equations, the inverse kinematic calculations were concluded.

## 8.2 Implementation

During the process of working with and testing several movement control options on the slave, many of the slave system shortcomings mentioned in section 6 caused problems. These included the extra weight and inertia added by the motors of the SSM, the weight and inertia of the PSM assembly, the lack of robot stiffness, the limited range (due to physical constraints) of most joints and the fundamental flaws in the PSM's spherical wrist design. These problems led to several constraints being put on the control system, which resulted in the final control structure not adhering to the one specified by figure 9.

In order to still demonstrate control of the robot by the joystick and to satisfy the main objective despite all of the constraints, the control setup was divided into two main modes of operation. For the first operational mode all the aspects pertaining to the left hand side of figure 9 was covered, but only position tracking of the robot end effector by moving the SSM motors was done. The orientation tracking was not executed in this operational mode, because complete functionality of the spherical wrist was needed, which was not the case. However, calculations to determine the required orientation could still be done.

The second operational mode was then used to show the ability to control those PSM joints that were in a working condition at the time of control execution. This control setup used a DOF to DOF approach, where a direct relation between the movements of the respective spherical wrist joints on the joystick and their counterparts on the robot was established. The effect of these two operational modes was that the first one could be used for larger movements, while the second one allowed relatively smaller movements and orientation changes.

Further aspects for control included the addition of pushbuttons to enable switching the individual master joint brakes on or off at any time, to enable zeroing of the slave at any time and to enable switching between the two main operational modes.

## 8.3 Simulation

To determine whether the modelling, encoder values, forward kinematics and working volume calculations were correctly executed and to serve as an error detection tool

during the course of the control system design process, custom simulation software was created. This entailed creating a MATLAB graphical user interface (GUI) that could display the position of the joystick joints (according to the encoder information) in real time. Figure shows the general form of the GUI. It was tested successfully when the drawn joints showed the same positions and orientations as those of the physical joystick.

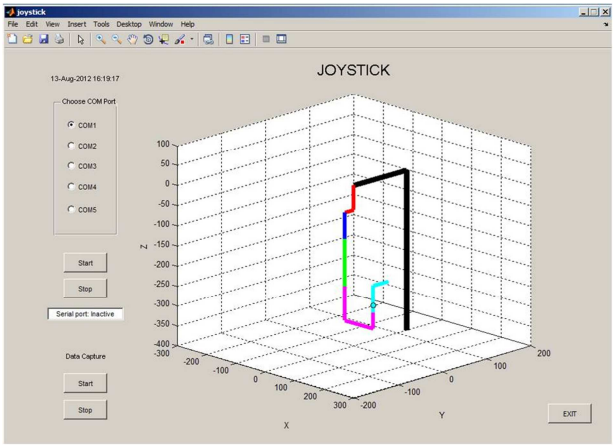


Figure 11: The joystick simulation GUI

This GUI was extended to include a robot simulation option. The working volume scaling could be done to determine the required robot end effector position and orientation, after which the inverse kinematics calculations could be executed to draw the simulated robot in real time. It provided an effective way to check calculations and test control options during the course of designing the two operational modes. It was also used as a safety precaution to test if control structures were satisfactory before actually applying it to the physical robot.

With the SSM and PSM not functioning as required, the desired control system from master to slave could not be demonstrated on the robot. In this case, the GUI was used to demonstrate the required control structure according to the specifications of figure 9. The new aspects of the GUI contain equations to incorporate the scaling factor and determine the $S\text{-}o_Rx_Ry_Rz_R$ reference frame. From the joystick's forward kinematics equations (equations 1 through 12) it then found the robot end effector's required position and orientation in this reference frame and consequently in the robot's base reference frame, $S\text{-}o_0x_0y_0z_0$. It then used kinematic decoupling and inverse kinematics (equations 12 through 25) to determine the required joint positions of the robot's spherical wrist. Once these variables were known, the robot could be drawn in real time.

The GUI was used to effectively demonstrate control of the slave system by the joystick, showing that the objective of controlling the seven DOF robot was satisfied. If it were not for the problems with the SSM and PSM this control system could have been demonstrated physically as well.

## 9. Testing

Tests were conducted to determine how well the master could control the slave's movement (i.e. movement control tests) to and from specific points within the robot working area. These tests also served to determine the intuitiveness level of the user interface (i.e. intuitiveness tests) and to provide technical specification of the master system.

### 9.1 Procedure

A simple PCB with two tactile switches (130 mm apart), each with a 10 mm x 10 mm pad, and two indicator LEDs was constructed and placed within the robot working volume, while the robot end effector was also positioned at its starting position (as per operational mode 1) in the working volume. Figure 12 shows the PCB.

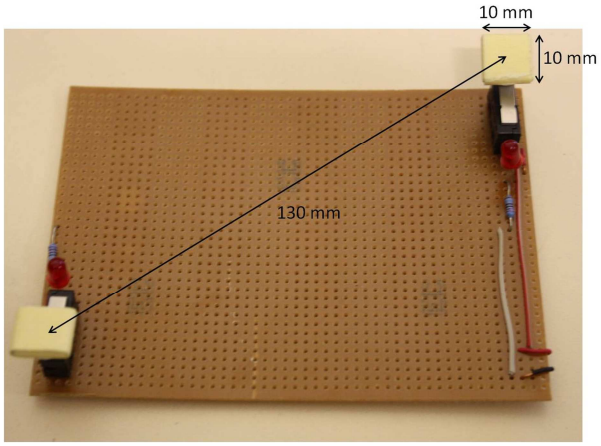


Figure 12: The testing PCB with its two pushbuttons

For all tests, the same basic procedure was executed: the slave was zeroed and moved to its operational mode 1 starting position; the joystick was used to move the robot end effector to the first switch pad and, when the LED flashed, Time_1 was documented as the duration of execution for this movement; the joystick was used to move the robot end effector to the second switch pad and, when the LED flashed, Time_2 was documented as the duration of execution for this movement. Figure 13a – c demonstrate these three parts of the procedure.

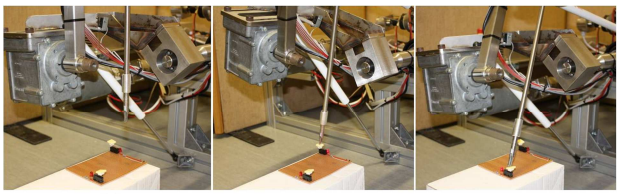


Figure 13: The testing procedure, showing the three positions

This procedure was executed 20 times by the designer of the system to provide expert data for the movement control tests. For the intuitiveness tests, four random subjects that have no experience with this or other similar master-slave controllers were each given a 5 min introduction on the functioning of the joystick and the specifics of movement control, which included the working volume orientation and the safety switch. The subjects were also allowed a 5 min practicing period to get accustomed to how the joystick operates. After this, a set of five tests were conducted by each subject, using the same method as explained above and again documenting Time_1 and Time_2.

### 9.2 Results

The results from the one set of 20 movement control tests and from the four sets of 5 intuitiveness tests are shown in figure 14 a through c.

Figure 14a shows Time_1 and Time_2 data for all 20 movement control tests, with the Time_1 average (7.93 s) indicated by the blue line and the Time_2 average (14.15 s) indicated by the red line. For each test the two switches were pressed successfully, indicating successful movement control tests.

Figure 14b shows the Time_1 data for the four sets of intuitiveness subject tests, as well as the subject average of 8.15 s and the expert average for Time_1 taken from figure 10a. Similarly, figure 14c shows the Time_2 data for the four sets of intuitiveness subject tests, as well as the subject average of 15.6 s and the expert average for Time_2 taken from figure 14a.

These subject averages compare very well with the respective expert averages of 7.93 s and 14.15 s from the movement control tests, which points to a very intuitive system. With little knowledge of the joystick, only a short introduction and minimal practice, the subjects executed movement control and sometimes even outperformed the expert data. This indicates successful intuitiveness tests. Subject feedback included the following: the joystick is easy to operate, the movement scale from joystick to robot is well defined and the safety button functionality is effective.

## 10. Discussion and Conclusion

This paper presented the design, construction and testing of a joystick-type master system for the execution of control on an existing seven DOF minimally invasive surgical robot. To this end, several tasks were executed in order to satisfy the main requirements of the final product.

A full understanding of the field of robotic surgery, specifically with regards to user interface systems, was achieved by means of researching current surgical robots and their specific designs. A detailed overview of the PSM and SSM systems was also given.

The iterative concept development process led to a final chosen design that, upon assembly, adhered to all of the engineering specifications that were set for it: it provided unhindered and intuitive movement (controlled by one hand) in a 30 cm x 30 cm x 30 cm working volume and its design was not constrained specifically to the SSM-PSM system. It allowed, with downscaling, a 10 cm x 10 cm x 10 cm 'safe space' of operation at the robot end.

The electromagnetic brakes allowed each of the joystick joints to be actuated independently – allowing direct control of the PSM motors – and the safety switch was incorporated successfully. The testing section supported the conclusion of an intuitive system by showing that subjects needed minimal preparation time and minimal understanding of the system's functional operation, before being able to control the robot optimally. An easy, low cost and accurate encoder was found in the AS5040 rotary magnetic encoder chip and its accompanying magnet. The electronic circuitry was successfully implemented, PCBs were created and mounted on each joint of the joystick and the software allowed 1024 positions per revolution to be sampled, which is more than the 1005 positions needed to satisfy the surgical robot resolution requirement. Although not fulfilling the suture resolution requirement of 10050 positions per revolution, the AS5040 chip provided enough resolution to demonstrate the functionality of the joystick accurately.

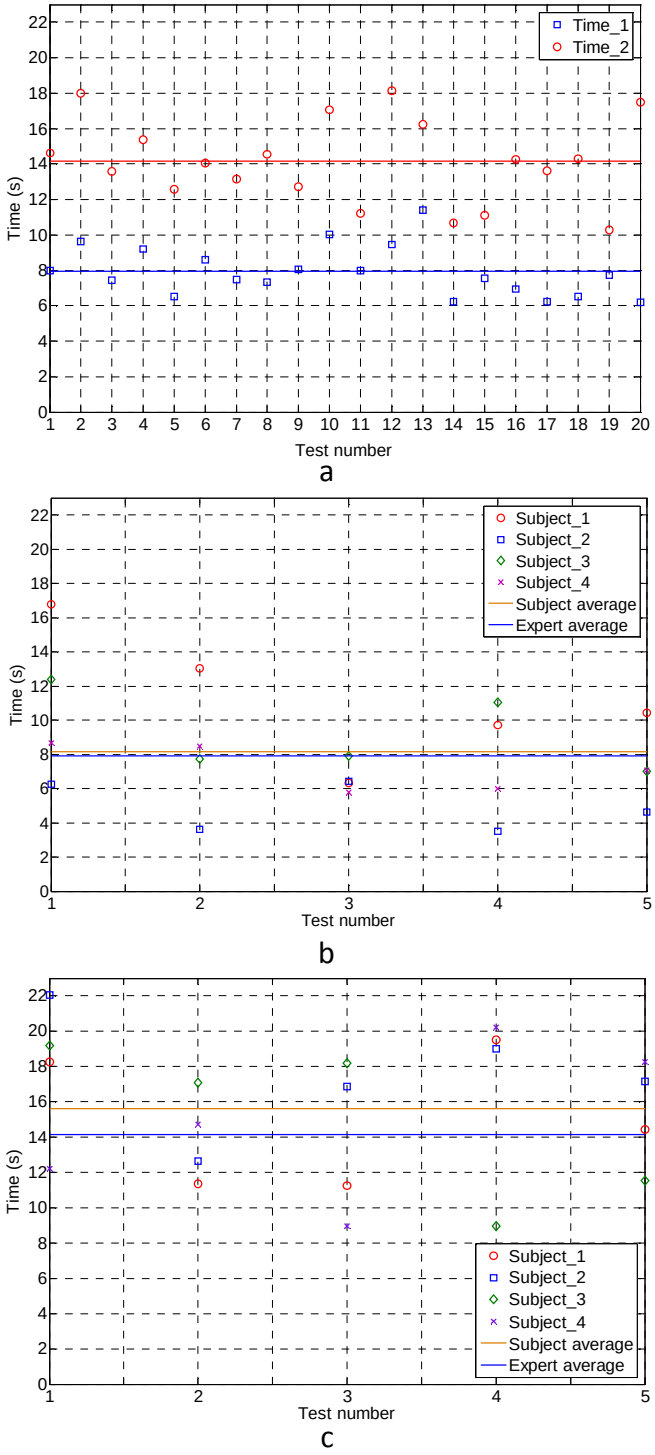


Figure 14: (a) Time data for the 20 movement control tests
(b) Time_1 data for the five intuitiveness tests conducted by four subjects
(c) Time_2 data for the five intuitiveness tests conducted by four subjects

 

The master and slave systems were interfaced successfully, with some shortcomings noted. Fundamental flaws in the mechanical design of both the PSM (with regards to the spherical wrist design, the cables and the strong motors) and SSM (with regards to the system's inertia and lack of stiffness) influenced the joystick's ability to control the robot's movement.

The control system design consisted of several aspects: firstly, the joystick and the robot were mathematically modelled according to the DH convention. Forward kinematic calculations were then applied to the joystick to determine its end effector position and orientation with respect to the joystick's base reference frame. These quantities were recalculated with respect to the joystick working volume, which could be scaled down to the robot working volume. From there, the desired position and orientation of the robot end effector was calculated with respect to the robot's base reference frame, which finally enabled calculation of the robot's required joint variables through inverse kinematics. This process was successfully demonstrated with the MATLAB GUI that was created for simulation and testing purposes.

A novel aspect that emerged from this control section is the functioning of the safety switch and its joystick working volume. To keep the robot stationary while the safety switch is released and to move the robot from that precise stationary point when the safety switch is pressed, a new algorithm was developed. It keeps the joystick working volume locked to the joystick's end effector while the safety switch is pressed and it locks the joystick working volume with respect to the base frame while the switch is released. This implies that movement inside the joystick working volume (which directly translates to the required movement in the robot working volume) is only registered when the safety switch is pressed. Research showed that only the MiroSurge system makes use of a similar functionality with its user interface[8].

Other comparisons with current technologies showed that the slave system design corresponded to that of the RAVEN's, with its motors situated outside the robotic arms, and that the surgical working volume concept satisfies the same "no-go zone" principle addressed by with the premapping function of the MiroSurge[8]. The scope of this paper did not extend to the haptic and visual feedback aspects of the user interface, which prevents further comparisons to other surgical robot systems. To increase functionality, accuracy and reliability, the addition of these platforms is recommended for future work

Testing was done to demonstrate the joystick's ability to control the robot. By using the joystick to move the robot end effector between two points, and doing this multiple times at relatively high speeds, it was shown that the joystick could successfully control the surgical robot's movement. Through similar tests, done by random subjects achieving highly comparable results, the system proved to be very intuitive.

## Acknowledgments

The authors would like to thank the Stellenbosch University Hope project for the support with funding provided.

## References

1. *Mack MJ*, Minimally invasive and robotic surgery, *The Journal of the American Medical Association*, 2001, 285(5), 568-572.
2. *Childress VW*, Robotic surgery, *The Technology Teacher*, 2007, 66(5), 9-13.
3. *Dai JS*, Surgical robotics and its development and progress, *Robotica*, 2010, 28, 161.
4. *Camarillo DB, Krummel TM and Salisbury JK*, Robotic technology in surgery: past, present and future, *The American Journal of Surgery*, 2004,188, S2-S15.
5. *Christiane P-J, Schreve K and Scheffer C*, Development of a minimally invasive robotic surgical manipulator. *R & D Journal of the SAIMechE, 2010*, 26, 27-33.
6. *Worst SC*, Development of a Low Cost Secondary Slave Manipulator for a Minimally Invasive Robotic Surgical System, Unpublished MSc Eng Thesis, Department of Mechanical and Mechatronic Engineering, Stellenbosch University, 2012.
7. *Intuitive Surgical Inc*., http://www.intuitivesurgical.com/ , 2012.
8. *Simorov A, Otte RS, Kopietz CM and Oleynikov D*, Review of surgical robotics user interface: what is the best way to control robotic surgery?, *Surgical Endoscopy*, 2012, 26, 2117–2125.
9. *Tavakoli M, Patel RV and Moallem M*, A force reflective master-slave system for minimally invasive surgery, *Proceedings of the IEEEIRSI International Conference on Intelligent Robots and Systems*, Las Vegas, Nevada, October 2003, 3077-3082.
10. *Sensable Technologies*, http://www.sensable.com/ , 2012.
11. *Phee SJ, Low SC, Huynh VA, Kencana AP, Sun ZL* and *Yang K*, Master and slave transluminal endoscopic robot (MASTER) for natural orifice transluminal endoscopic surgery (NOTES), *31st Annual International Conference of the IEEE EMBS*, Minneapolis, Minnesota, USA, 2-6 September 2009, 1192-1195.
12. *Van den Bedem L, Hendrix R, Rosielle N, Steinbuch M* and *Nijmeijer H*, Design of a minimally invasive surgical teleoperated master-slave system with haptic feedback, *Proceedings of the IEEE International Conference on Mechatronics and Automation* Changchun, China. 9-12 August 2009, 60-65.
13. *Spong MW, Hutchinson S* and *Vidyasagar M*, Robot Modelling and Control, 1st edition, Hoboken: John Wiley & Sons Inc., 2006.
14. *Lobontiu A* and *Loisance D*, Robotic surgery and tele-surgery: basic principles and description of a novel concept, *Journal de Chirurgie* 2007, 3(3), 208-214.
15. *Miki-Pulley*, http://www.mikipulley.co.jp , 2012.
16. *Austria Microsystems*, http://www.ams.com/eng/ , 2012.
17. *Arduino.* http://arduino.cc/ , 2012.